Available online at www.sciencedirect.com
SCIENCE DIRECT®
Journal of Sound and Vibration 272 (2004) 1013–1032
JOURNAL OF SOUND AND VIBRATION
www.elsevier.com/locate/jsvi

An experimental technique for complete dynamic characterization of a viscoelastic material

R. Caracciolo[a], A. Gasparetto[b,*], M. Giovagnoni[b]

[a] *Dipartimento di Tecnica e Gestione dei Sistemi Industriali, Università di Padova, Stradella S. Nicola, 3, I-36100 Vicenza, Italy*

[b] *Dipartimento di Ingegneria Elettrica, Gestionale e Meccanica, Università di Udine, Via delle Scienze, 208, I-33100 Udine, Italy*

Received 28 October 2002; accepted 26 March 2003

Abstract

An experimental technique for completely characterizing a viscoelastic material, by determining the Poisson ratio and the complex dynamic Young's modulus of a small beam-like specimen subject to seismic excitation is presented in this paper, together with the theoretical background.

The same experimental device is used basically for both kinds of tests: the specimen is instrumented, placed into a temperature controlled chamber and excited by means of an electrodynamic shaker. The longitudinal and the transversal deformations are measured by strain gauges to get the Poisson ratio, whereas the vertical displacement of the specimen and the acceleration of the support are measured to get Young's modulus of the tested material.

The experimental curves of the Poisson ratio and of Young's modulus, obtained at different temperatures, are then gathered into a unique master curve by using the reduced variables method. The two master curves, respectively, represent the Poisson ratio and Young's modulus for the tested material in a very broad frequency range.

1. Introduction

According to the theory of viscoelasticity [1–3], knowledge of two parameters is required in order to have a complete dynamic characterization of the mechanical behaviour of an isotropic viscoelastic material.

*Corresponding author. Tel.: +39-0432-558257; fax: +39-0432-558251.
E-mail address: gasparetto@uniud.it (A. Gasparetto).

0022-460X/$ - see front matter © 2003 Elsevier Ltd. All rights reserved.
doi:10.1016/j.jsv.2003.03.008

The usual procedure consists of measuring two moduli (e.g., the elasticity and the shear modulus) or one modulus and the Poisson ratio of a viscoelastic material, through ad hoc experimental tests carried out at different temperatures. It is also well known that such parameters have a certain dependence on many environmental and operating conditions, but mainly on frequency and temperature.

A short review of the experimental work on the measurement of the dynamic parameters of a viscoelastic material is presented in the following.

Gottenberg and Christensen [4] measured the complex shear modulus of a linear, isotropic, viscoelastic solid and determined its dependence on frequency and temperature.

The work by Pritz [5–8] is of primary importance. He evaluated the complex modulus of acoustic materials using a transfer function method, namely by exciting a cylindrical or prismatic specimen at one end, the other end being loaded by a mass, and by modelling the specimen by lumped mechanical elements. In this way the transfer function of the specimen from the excited end to the loaded one could be determined.

Holownia [9] employed a technique, based on holographic interferometry, to measure the dynamic Young's modulus for rubbers. Holownia and Rowland [10] used the electronic speckle pattern interferometry (ESPI) technique to obtain a measurement of the dynamic bulk modulus for rubbers, by gauging the volume contractions of submerged specimens subjected to sinusoidal pressure changes.

Sim and Kim [11] managed to estimate the properties of viscoelastic materials for finite element method application, by means of a technique based on theoretical considerations as well as on data obtained from transmissibility measurements.

Ödeen and Lundberg [12] measured the endpoint accelerations of an impact-loaded rod specimen and, by applying an iterative numerical scheme, obtained quantitative values for the complex modulus of a linearly viscoelastic material. Trendafilova et al. [13] measured the displacements, instead of the accelerations, of the specimen ends by means of electro-optical transducers to get the same results.

A major problem with this kind of experimental tests is that the frequency range of the measurement is often quite narrow, since the techniques used do not allow the values of the parameters to be obtained directly in a broad frequency range. Recently, some techniques have been proposed and applied to overcome this problem, as for instance those based on quasi-static methods and on ultra-sound methods [14,15].

Another approach to greatly enlarge the frequency range of measurement is based on the so-called "method of reduced variables" [2]. This technique is based on the time–temperature superposition hypothesis: in other words, the behaviour of any viscoelastic parameter at a given temperature over a broad range of frequency can be obtained by suitably combining the plots of that parameter, at different temperatures and over narrower frequency ranges.

The present work describes the determination of both the Poisson ratio and Young's modulus for some viscoelastic material (a mixture of PVC and calcium carbonate used for industrial purposes) which was at our disposal.

The paper is organized as follows. First, the theoretical framework used as a basis for the experimental measurement of both moduli is presented. To begin, the definition of the Poisson ratio is given, first in the time domain and then in the frequency domain by means of complex numbers. Next, the theory behind the experimental tests for the measurement of Young's modulus

is presented. Such theoretical background turns out to be much more complicated than the one for the Poisson ratio, because a formula explicitly expressing Young's modulus in terms of measurable entities is needed.

Then, the experimental set-up for the two series of tests is described. The same set-up (i.e., a specimen of the viscoelastic material mounted on a support and excited by an electrodynamic shaker placed inside a temperature controlled chamber) has basically been used for both types of tests, the differences lying in the type of entities that are measured, as well as in some experimental conditions (as the type of boundary conditions to which the specimen is subject). Namely, the longitudinal and the transversal deformations are measured by strain gauges to get the Poisson ratio, whereas the vertical displacement of the specimen and the acceleration of the support are measured by a laser sensor and an accelerometer to get Young's modulus.

In this way, the values of the two moduli for the material under test, at a certain temperature and over a small frequency range, were obtained. The test was then repeated for different temperatures, so as to obtain a set of curves for the Poisson ratio and another set for Young's modulus. Each set of curves was then gathered into a unique master curve by using an iterative procedure based on the reduced variables method. In other words, the causality condition, which relates the absolute value to the phase angle of any complex parameter of a causal system, was used to determine the shifts that should be applied to the curves at the different temperatures in order to obtain a unique master curve at a reference temperature. The two master curves thus obtained respectively represent the Poisson ratio and Young's modulus for the viscoelastic material in a very broad frequency range.

A more detailed theoretical background, as well as some partial results of the work done by the authors of this paper during many years of work on this topics, can be found in Refs. [16–20].

2. Theory of the Poisson ratio

For a viscoelastic material, the Poisson ratio $\nu(t)$ can be defined [1] as the opposite of the ratio of the lateral strain $\varepsilon_y(t)$ to the constant axial strain $\varepsilon_x(t)$, under uniaxial stress relaxation conditions. In other words, $\nu(t)$ is the lateral strain due to a unit step of longitudinal strain. Hence, in uniaxial stress conditions the lateral strain can be obtained from the axial strain through a convolution integral:

$$\varepsilon_y(t) = -\int_{-\infty}^{t} \nu(t-\tau)\,\frac{\mathrm{d}\varepsilon_x}{\mathrm{d}\tau}\,\mathrm{d}\tau. \tag{1}$$

In order to obtain an expression in the frequency domain, $\nu(t)$ can be split into a constant term and a time-varying term, which becomes zero for t approaching infinite:

$$\nu(t) = \nu_\infty + \hat{\nu}(t) \quad \text{where } \hat{\nu}(t)\to 0 \text{ for } t\to\infty. \tag{2}$$

Substituting Eq. (2) into Eq. (1), introducing complex numbers to represent periodic entities of the type $\varepsilon(t) = \varepsilon_0 \mathrm{e}^{\mathrm{i}\omega t}$, and making the change of variable $(t-\tau) = \eta$, the expression of ν in the frequency domain can be obtained:

$$\nu(\mathrm{i}\omega) = -\frac{\varepsilon_y(\mathrm{i}\omega)}{\varepsilon_x(\mathrm{i}\omega)}, \tag{3}$$

where the complex the Poisson ratio $v(i\omega)$ is defined, with respect to the corresponding relaxation function, as

$$v(i\omega) = v_\infty + i\omega \int_0^\infty \hat{v}(\eta) e^{-i\omega\eta} \, d\eta. \tag{4}$$

As it can be seen from Eq. (3), $v(i\omega)$ can be directly obtained from measurements of the longitudinal and transverse strains at each frequency in uniaxial stress conditions. Thus, for the Poisson ratio there is no need to further elaborate the above expressions.

A beam in bending provides a good experimental approximation to uniaxial stress. Hence, a specimen of the considered material can be built, that implements a beam which is excited by an electrodynamic shaker generating a sinusoidal seismic wave. Then, longitudinal and transverse strains can be measured at the same location by means of a couple of strain gauges (each one is composed of two perpendicular superimposed grids) located on the upper and lower face of the beam.

In order to keep the stress distribution as near as possible to uniaxial conditions, the so-called "plate-effect" of the beam must be considered. In fact, the wider the beam, the smaller the transverse strain, and if the beam degenerates into an infinitely wide strip, then the transverse strains will always be zero and plain strain conditions will hold.

The plate effect is especially to be considered in tests at different frequencies, since if the input frequency increases, the response of the system is more and more influenced by higher modes. In a simply supported beam, higher modes correspond to smaller distances between zeroes of the eigenfunctions, which can be considered equivalent to shortening the specimen.

An important consideration, which will affect the placement of the strain gauges on the specimen, is that if a beam is excited by a shaker, only odd modes appear in the response because the inertia loading is constant along the beam. Thus, if the strain gauges are placed at a distance from a support which is equal to one third of the length of the beam, then the third mode and some higher odd modes (like the ninth etc.) do not affect the measurement, because the sensor location corresponds to a zero of the eigenfunction. Under these conditions, the strains measured at one third of the beam length are due to the first, fifth, seventh, eleventh, etc., mode. A sketch of the beam-like specimen showing the gauge location, the geometric parameters of the beam and the used reference system is reported in Fig. 1.

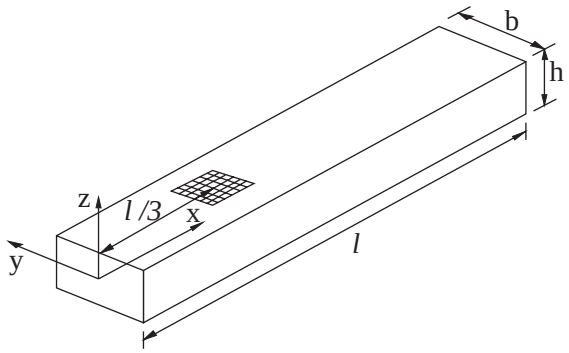

Fig. 1. Specimen characteristics for measurement of the Poisson ratio.

We define now the "apparent" the Poisson ratio as the opposite of the ratio between the transverse and the longitudinal strains measured at one third of the length of the beam:

$$v_a(\ell/b, \mathrm{i}\omega) = -\frac{\varepsilon_y(x = \ell/3, \mathrm{i}\omega)}{\varepsilon_x(x = \ell/3, \mathrm{i}\omega)}, \tag{5}$$

which is a function of frequency and of the length-to-width ratio of the specimen. Following such a definition, the error in the measurement of the absolute value of the Poisson ratio can be written as

$$error(\ell/b, \mathrm{i}\omega) = |v_a/v - 1|. \tag{6}$$

Giovagnoni [16] proved that, if the input frequency is less than 1.41 times the resonance frequency of the beam, there is an upper bound to the error defined in Eq. (6).

Referring to the tests for the Poisson ratio carried out by the authors, the beam-like specimen is 0.1 m long and 7 mm wide, and the distance ℓ between the supports is 95 mm, thus yielding a ℓ/b ratio equal to 13.571. Hence, if the input frequency is less than 1.41 times the resonance frequency, it results that the maximum error due to the plate effect is 2.6%. This means that the absolute value of the measured the Poisson ratio, i.e., the apparent the Poisson ratio as defined in Eq. (5), will decrease in this frequency range due to the plate effect, and this erroneous decrease will be limited to 2.6%.

3. Theory of Young's modulus

It will be shown in this section that Young's modulus can be obtained through experimental measurements in a beam-like specimen seismically excited by a sinusoidal force input, namely by simultaneously measuring the vertical displacement of a suitable point of the bending beam and the acceleration of the supporting basement.

The definition of Young's modulus, as well as its representation as a complex number, is quite similar to that of the Poisson ratio given in the previous section. First, it should be recalled that the relaxation modulus $E(t)$ for an isotropic material is defined as

$$\sigma(t) = \int_{-\infty}^{t} E(t-\tau)\,\frac{\mathrm{d}\varepsilon(\tau)}{\mathrm{d}\tau}\,\mathrm{d}\tau, \tag{7}$$

where $\sigma(t)$ is the stress and $\varepsilon(t)$ the strain in condition of uniaxial stress relaxation conditions. The strain history can be specified as a harmonic function of time $\varepsilon(t) = \varepsilon_0 \mathrm{e}^{\mathrm{i}\omega t}$, while $E(t)$ can be split into the sum of an asymptotic constant term E_∞ and a time-variable one $E'(t)$:

$$E(t) = E_\infty + E'(t), \tag{8}$$

where $E'(t) \to 0$ as $t \to \infty$. Such a decomposition is necessary to obtain an expression for the complex Young's modulus whenever the viscoelastic body is subjected to steady state oscillatory conditions. As for the Poisson ratio, Young's modulus in the frequency domain can be expressed by

$$\sigma(t) = E_\infty \varepsilon_0 \mathrm{e}^{\mathrm{i}\omega t} + \mathrm{i}\omega\varepsilon_0 \int_{-\infty}^{t} E'(t-\tau)\,\mathrm{e}^{\mathrm{i}\omega t}\,\mathrm{d}\tau, \tag{9}$$

which becomes, after setting $t-\tau=\eta$:

$$\sigma(t)=\left[E_\infty+\mathrm{i}\omega\int_0^\infty E'(\eta)\,\mathrm{e}^{-\mathrm{i}\omega\eta}\,\mathrm{d}\eta\right]\varepsilon_0\mathrm{e}^{\mathrm{i}\omega t}. \tag{10}$$

To be consistent with the steady state conditions assumed for strain history, the stress will be taken to have the same steady state form:

$$\sigma(\mathrm{i}\omega)=E(\mathrm{i}\omega)\,\varepsilon_0\mathrm{e}^{\mathrm{i}\omega t}, \tag{11}$$

which gives Young's modulus as a ratio between complex numbers:

$$E(\mathrm{i}\omega)=\frac{\sigma(\mathrm{i}\omega)}{\varepsilon(\mathrm{i}\omega)}. \tag{12}$$

Hence, the complex Young's modulus $E(\mathrm{i}\omega)$ eventually results:

$$E(\mathrm{i}\omega)=E_\infty+\mathrm{i}\omega E'(\mathrm{i}\omega). \tag{13}$$

However, Eq. (13) cannot be practically employed, since stress measurements cannot be easily and accurately performed. It is therefore necessary to obtain an expression for Young's modulus suitable for experimental measurements that can actually be performed in a laboratory. To this aim, the theory of seismically excited beams should be employed. The theoretical procedure to get this expression for Young's modulus has been proved in a previous paper by Caracciolo et al. [19], so only the most important considerations and the final results will be reported here.

The crucial point is to express the modal co-ordinate used for decoupling the equation of a seismically excited beam as a function of an entity that can be experimentally measured. At the beginning, the first idea of the authors, in order to measure the strain at a suitable point of the specimen, was to employ a strain gauge, as done for measuring the Poisson ratio. However, the results of the tests were not satisfactory because the glue used to fasten the gauge to the specimen stiffened the viscoelastic material, thus heavily affecting the measurements. The idea was then to use a contactless laser sensor, that measures the absolute local vertical displacement of the specimen. Therefore, the modal co-ordinate is to be expressed as a function of the absolute displacement u_L measured by the laser sensor.

A way to approximate the eigenfunction expansion with only the first term can be done by positioning the laser at a distance d from the clamped edge of the beam, such that the second eigenmode is not excited, and by neglecting the higher order modes (it has been shown by Caracciolo et al. [19] that the error due to the third mode is less than 0.32%, and it decreases rapidly with the order increase). Thus, after some algebra, the final expression obtained is

$$E(\mathrm{i}\omega)=\frac{\rho L^4}{h^2}\left[F_1\left(\frac{u_L(\mathrm{i}\omega)}{a_b(\mathrm{i}\omega)}+\frac{1}{\omega^2}\right)^{-1}+F_2\omega^2\right] \tag{14}$$

where ρ is the material density, L is the beam length, h is the beam depth, u_L is the absolute displacement measured by the laser sensor, a_b is the acceleration of the base of the support of the beam, and the dimensionless parameters F_1 and F_2 are computed according to the theory of beams. Namely, by applying Eq. (14) to the case of a cantilever beam, the expression to get

Young's modulus of the tested specimen becomes:

$$E(\mathrm{i}\omega) = \frac{\rho L^4}{h^2}\left[-1.0686\left(\frac{u_L(\mathrm{i}\omega)}{a_b(\mathrm{i}\omega)} + \frac{1}{\omega^2}\right)^{-1} + 0.9707\omega^2\right]. \tag{15}$$

4. Experimental set-up and measurement results for the Poisson ratio

In order to measure the Poisson ratio, the specimen of the viscoelastic material (a mixture of PVC and calcium carbonate) is mounted (under "pinned–pinned" conditions) to a support placed on an electrodynamic shaker. Special care had to be taken in order to ensure the following test conditions:

(1) the modifications in the input acceleration due to resonances of the base carrying the specimen had to be minimized; (2) the mechanical loading effect due to the wires connecting the strain gauges had to be minimized; (3) the friction in the supports had to be minimized. This was done by making each support with two coaxial counteracting screws with conical points.

The wires connecting the strain gauges are very thin insulated wires (those usually employed in the micro-motor coils) that are connected to a small plate fixed inside the base. In this way, the quality of the measurements could be significantly improved, by increasing the low signal-to-noise ratio.

The scheme of the measurement system for the Poisson ratio is reported in Fig. 2(a).

The sensors used in the tests are Micro Measurements CEA-06-125WT-350 strain gauges connected to Hottinger–Baldwin KWS 3082A carrier amplifiers (carrying frequency 5 kHz). Each gauge is made by means of two superimposed orthogonal grids with two sensors located on the upper and lower side of the beam, so as to compensate the signal with respect to temperature changes. The two signals of the transverse and lateral strain are then input into a National Instruments AT2150C plug-in board for analogue-to-digital conversion.

All tests at different temperatures were carried out by slowly sine-sweeping the input acceleration of the base. The longitudinal strain was kept to a constant value (about 15 με) during the sweep by using the corresponding signal as the feedback input for the sweep controller. No linearity problems were observed: the results were shown to be independent from the strain level.

The temperature controlled chamber is implemented by means of a closed air circuit, made of a fan forcing the air through a cooling panel and a heating resistance. The temperature distribution in the air flow is homogenized by means of a honeycomb panel before reaching the specimen. The temperature control is obtained by keeping the cooling element on and by adjusting the current through the heating resistance. The value of the air temperature is measured near the specimen and a simple proportional gain is used to drive the heating element. The whole set-up has been brought to stationary conditions before each test.

Measurement results are shown in Fig. 3 with the corresponding test temperatures. The plots show the absolute value of the Poisson ratio in the frequency interval 75–530 Hz. It can be noted that all the functions shown in Fig. 3 decrease with frequency. A first remark is that, as the temperature increases, the absolute value of the Poisson ratio also increases. A second remark is that the slope of the curves increases at higher temperatures. However, it should be noted that the

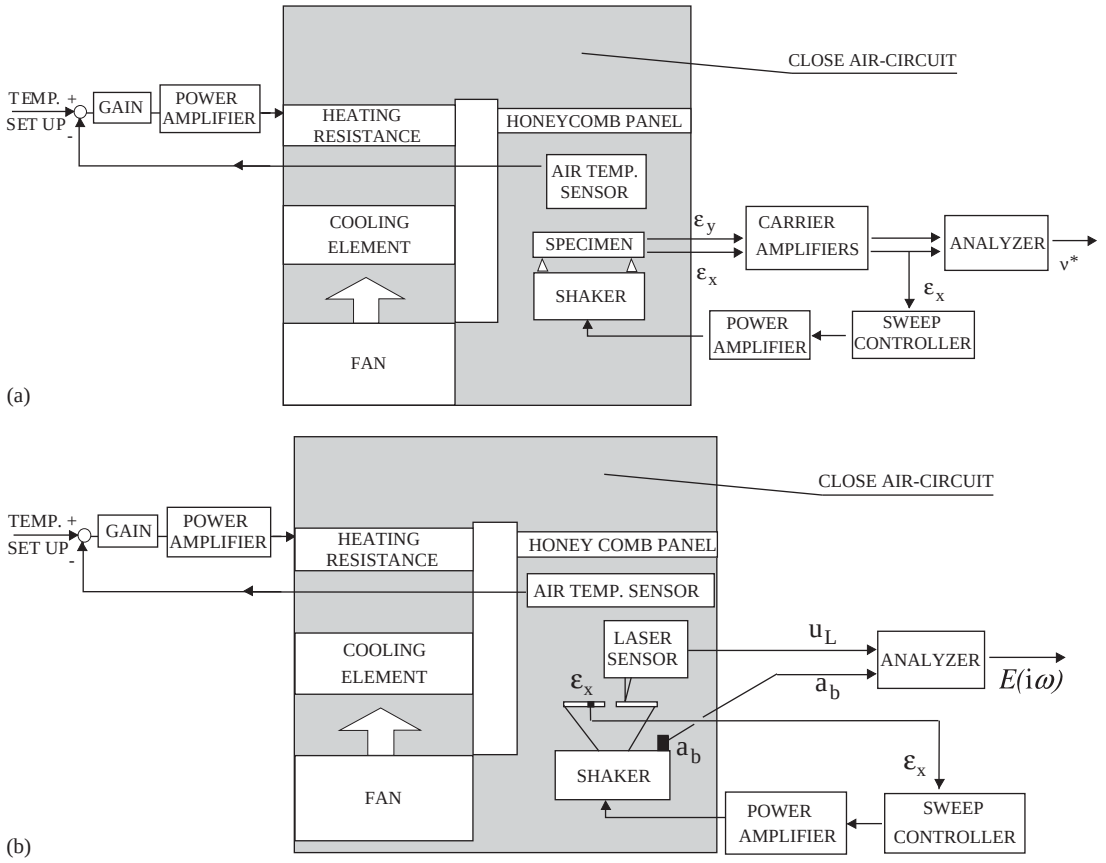

Fig. 2. Schematic diagram of the whole measurement system (a) for the Poisson ratio; (b) for Young's modulus.

curves in Fig. 3 are quite flat and this requires special care when overlapping them to determine the frequency shifts, according to the procedure described in the next Section.

5. Application of the reduced variables method for determination of the master curve of the poisson ratio

The "reduced variables method" [2,3] states that all the curves of a specific modulus of some material at different temperatures, like those of the Poisson ratio reported in Fig. 3, can be gathered in a single plot, the so-called "master curve", that accounts for the material property in a much broader frequency range. In other words, a unique plot of some viscoelastic property versus frequency at a given temperature T_0 can be obtained in logarithmic axes by shifting of an amount ($\log a_T$) every plot of the same viscoelastic property measured at a temperature T. The parameter $\log a_T$ is defined by the WLF equation:

$$\log a_T = -c_1^0(T - T_0)/(c_2^0 + T - T_0). \tag{16}$$

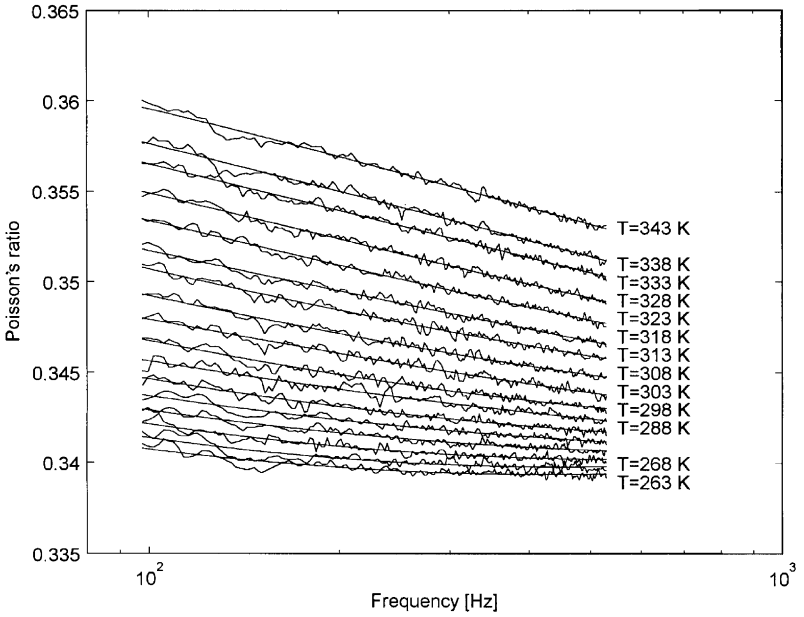

Fig. 3. Absolute values of the Poisson ratio obtained from the measurements at different temperatures (253–338 K), together with the interpolating parabolic functions.

The two constants c_1^0 and c_2^0 appearing in Eq. (16) depend on the temperature T_0 that was to reduce the plots (of course, they also depend on the considered material). Thus, by shifting the experimental curves taken at different temperatures, one can obtain a unique plot covering several decades of frequency. In order to determine c_1^0 and c_2^0, adjacent curves must be shifted so as to make them overlap. In this way one heuristically can build a first version of the master curve, and the shifts given to the curves enable one to find the values of c_1^0 and c_2^0. Unfortunately, this procedure cannot be practically used, because the errors in the shifts between adjacent curves at neighbouring temperatures add up continuously while trying to building the master-curve, so that the shifts of the experimental curves taken at temperatures very different from the reference temperature T_0 can be affected by severe errors. This problem becomes even more critical if the curves are flat (as in the case of the experimental plots of the Poisson ratio) because in this case small vertical displacements of the plots correspond to large horizontal displacements in overlapping; hence, large errors are very likely to occur.

As expected, a first attempt to build up the master curve using the heuristic procedure described in the foregoing did not give satisfactory results: the coefficients c_1^0 and c_2^0, obtained from heuristic shifts, resulted very different from those reported in the literature for polymers similar to the material under test.

Hence, a more sophisticated procedure had to be conceived. So, the following procedure based on a cross-verification of the shifts by means of a "causality criterion" was applied, and much better results were obtained.

The causality criterion on which the procedure is based can be expressed as follows. It should be remembered that the real part and the imaginary part of the frequency response of whatever

existing entity are not independent, since they are obtained from the same real function, i.e., the response to the unit impulse. In other words, the absolute value and the phase of any frequency response are related to each other, because otherwise anti-transformation of the frequency response would yield a non-zero impulse response before the initial instant $t = 0$, i.e., before the application of the input signal. Hence, such a system would be non-causal, as it would react before the application of the input, which is absurd for any system existing in the real world. For this reason, the relation existing between the absolute value and the phase of a frequency response is called "causality relation".

The Poisson ratio, a complex number, can be regarded as a frequency response with the longitudinal strain as input and the transverse strain as output. Thus, as for any frequency response, the causality condition must hold to ensure that the corresponding impulse response (or, as in Eq. (1), the unit-step response) in the time domain is a real function equal to zero before the application of the input. An approximate version of the causality condition relates the logarithmic derivative of the absolute value v to the phase angle φ of Poisson ratio in the form expressed by the so-called "Bode's theorem":

$$\varphi(\mathrm{i}\omega) \cong \frac{\pi}{2} \frac{\mathrm{d}\,\log|v(\mathrm{i}\omega)|}{\mathrm{d}\,\log\,\omega}. \tag{17}$$

Eq. (17) is also known as the "dispersion relation", namely the approximate, local version of the Kramers–Krönig relation, after the authors who developed them first in the theory of electromagnetic wave propagation. It must be kept in mind that such an approximation is suitable if one assumption holds, namely that the dynamic properties of the material are slowly varying functions of frequency, as discussed in Ref. [21]; hence, one has to be cautious when using the local Kramers–Krönig relation for calculation, because they are not exact.

The procedure to determine the shifts of the experimental curves in order to build the master curve will now be described. As it can be seen from Fig. 3, the plots of the absolute values of the Poisson ratio are quasi-straight lines and the corresponding phase plots do not show significant variations, as one can expect from Eq. (17). Thus, every experimental curve at a temperature T_i can be interpolated with a straight line for the absolute value and with a constant straight line for the phase angle, in accordance with Eq. (17). The shifts are then determined by overlapping the straight lines representing the absolute values by means of the least-squares method. At this stage of the procedure, a first master curve at the reference temperature T_0 is obtained in the form of a piece-wise straight line for the absolute values and a piece-wise constant plot for the phase angles in accordance with Eq. (17).

Eq. (17), if differentiated once more, yields:

$$\frac{\mathrm{d}\varphi(\mathrm{i}\omega)}{\mathrm{d}\,\log\,\omega} \cong \frac{\pi}{2} \frac{\mathrm{d}^2\log|v(\mathrm{i}\omega)|}{\mathrm{d}(\log\,\omega)^2}. \tag{18}$$

This relation suggests that the slope of the diagram of the phase angle corresponds to the curvature of the diagram of the absolute value. It is important to note that the slope of the phase plot is determined by the shifts, because the mean value of the slope can be obtained by dividing the phase difference between two neighbouring diagrams by the shift between the same two diagrams. Moreover, the mean value of the slope of the phase corresponds to the mean value of the curvature of the absolute value. Thus, a better interpolation of the absolute values is obtained

by using arcs of parabolas instead of straight lines. The overlapping procedure is then repeated for the parabolas in order to determine new shifts, which in turn enables one to update the values of the curvatures. This process is repeated until convergence is reached to the final shifts which will be used to build up the master curve. A direct application of this procedure to the experimental curves at hand showed that just few iterations are necessary to obtain stable shifts. The resulting values of the shifts enable one to obtain the c_1^0 and c_2^0 coefficients appearing in Eq. (16); the resulting values are in good agreement with those reported in the literature for Young's or shear modulus for polymeric materials.

For sake of clarity, the procedure is reported here step by step:

(1) a straight line is obtained through a least-squares fit of experimental data at temperature T_i:

$$|v_i| = \beta_i x + \gamma_i \quad \text{and} \quad \varphi_i = \frac{\pi}{2}\beta_i \ \text{ where } \ x = \log \omega;$$

(2) the absolute value and the phase in the midpoint x_m of the frequency-range of measurement are computed from:

$$|v_i(x_m)| = \beta_i x_m + \gamma_i \quad \text{and} \quad \varphi_i(x_m) \equiv \varphi_i = \frac{\pi}{2}\beta_i.$$

These values will be left unmodified during the whole procedure, as they are obtained directly from the measurements;

(3) the following steps are then repeated in the procedure (j is the iteration index):

(3.1) shifts $s_i^j = (\log a_T)_i^j$ for each plot at temperature T_i in the jth iteration are determined by overlapping the parabolic functions:

$$|v_i|^j = \alpha_i^j x^2 + \beta_i^j x + \gamma_i^j$$

by means of a least-squares fit between plots at adjacent temperatures. The values of α_i^j, β_i^j and γ_i^j are updated at every iteration, after letting $\alpha_i^0 = 0$; $\beta_i^0 = \beta_i$ and $\gamma_i^0 = \gamma_i$.

(3.2) if x_m is the same for all measurements, a mean slope of the phase at each temperature can be computed using the values of the shifts calculated at point 3.1:

$$\left(\frac{\mathrm{d}\varphi_i}{\mathrm{d}x}\right)^j = \frac{\varphi_{i+1} - \varphi_{i-1}}{s_{i+1}^j - s_{i-1}^j} = \frac{\pi}{2}\frac{\beta_{i+1} - \beta_{i-1}}{s_{i+1}^j - s_{i-1}^j}.$$

This mean slope determines the α parameter, i.e., the curvature, of the updated parabolas.

(3.3) It is now imposed that for $x = x_m$, the updated parabolas satisfy the curvature of point (3.2) and the slope and value of point (2). We obtain new values $\alpha_i^{j+1}, \beta_i^{j+1}, \gamma_i^{j+1}$ at the temperature T_i from the following relations:

$$2\alpha_i^{J+1} = \left(\frac{\mathrm{d}\varphi_i}{\mathrm{d}x}\right)^j,$$

$$2\alpha_i^{J+1} x_m + \beta_i^{J+1} = \varphi_i(x_m),$$

$$\alpha_i^{J+1} x_m^2 + \beta_i^{J+1} x_m + \gamma_i^{J+1} = |v_i(x_m)|.$$

These values can be employed again in step (3.1). Step 3 is repeated until no significant change is found in updating the curves. In our case, less then 10 iterations were enough to this purpose.

Fig. 3, together with the experimental curves, also shows the parabolas obtained at the end of the iterative procedure.

Reliable shifts are now available to build up the master curve. Applying a least-squares fit of $(T - T_0)/\log a_T$ versus $(T - T_0)$ the values $c_1^0 = 19.6$, $c_2^0 = 198.1$ for $T_0 = 278$ K are obtained. They are in reasonable agreement with the values reported in the literature for Young's or shear modulus of materials similar to that of the analyzed specimen.

The c_1^0 and c_2^0 coefficients can now be employed to build up the master curves of the absolute value and of the phase angle of the Poisson ratio. These master curves are shown in Figs. 4 and 5, respectively.

The master curve of the absolute value, shown in Fig. 4, needs no particular comment: the final result is good and shows that the absolute value of the Poisson ratio really decreases with frequency. Several decades of frequency are now available and this allows one to deduce that the decrease is true and not simply due to the plate effect of the specimen, as one could suppose.

The master curve of the phase angle, shown in Fig. 5, needs a deeper comment. As can be seen, the values of the phase angles are negative and very small (they vary between -1.2° and -0.1°). This remark agrees, as predicted by the causality condition, with the fact that absolute values decrease, but very slowly as the frequency increases. However, the slope of each phase plot should be positive to match the overall behaviour and this is not the case of Fig. 5. On the other hand, it should also be noticed that the variation of the value of the phase angle due to the negative slope is small, if compared to the mean value of each plot.

In other words, the mean values of the phase angles are in good agreement, also with the slope of the master curve of the absolute value, but the slopes are not. Thus, a reasonable hypothesis is that the error due to the plate effect of the specimen is not so severe as to modify the mean values,

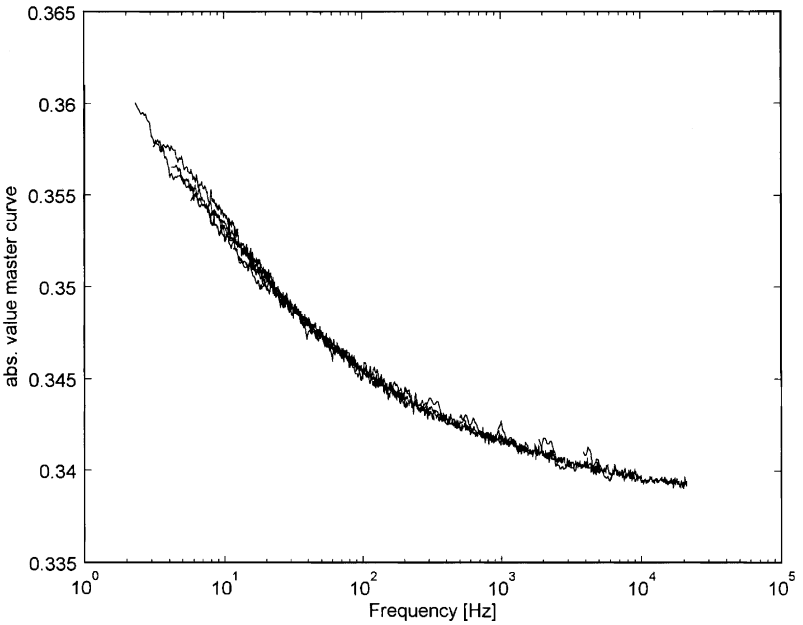

Fig. 4. Master curve of the absolute value of the Poisson ratio.

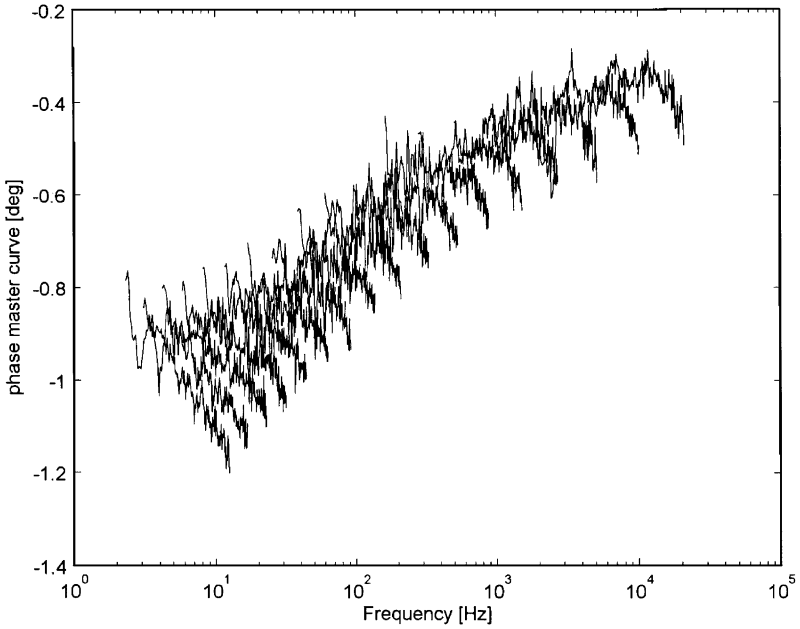

Fig. 5. Master curve of the phase angles of the Poisson ratio.

but it is important enough to change the slope of the plots of Fig. 5. In the plots of the absolute value, this effect corresponds to a small change in curvature, which plays no relevant graphical role in the overlaps of Fig. 4.

The procedure based on the causality criterion has produced reasonable coefficients for the WLF equation, while simple overlaps did not. However, modifying the curvature of the parabolas to satisfy the causality requirements corresponds to compensating the mismatching of the slopes in the phase-plots, and this process produces reasonable WLF coefficients. Thus, an error affects the slopes of the phases and this is probably due to the plate-effect of the specimen, which acts in the sense of emphasising the decrease of the complex the Poisson ratio with frequency.

6. Experimental set-up and measurement results for Young's modulus

The complex dynamic Young's modulus has been measured for the viscoelastic material using the procedure reported in the following. This procedure is based on the theoretical considerations carried out in Section 3. A beam-like specimen has been placed onto an ad hoc support and excited by an electrodynamic shaker that produces a vertical sine-sweep seismic force. A laser sensor measures the vertical displacement of a specific point of the beam, namely the nodal point for the second eigenmode, and a piezoelectric accelerometer measures the vertical acceleration of the base.

Fig. 6 shows the specimen characteristics, and Fig. 7 is a diagram of the set-up of the beam on the support, which in turn is placed onto the electrodynamic shaker. Fig. 8 is a picture of this experimental set-up. This apparatus is located inside a temperature controlled chamber, so as to

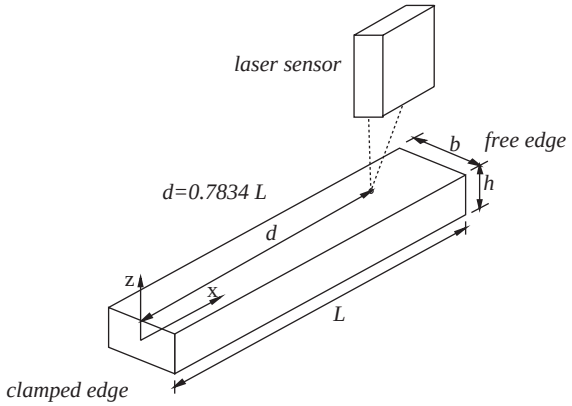

Fig. 6. Specimen characteristics for measurement of Young's modulus.

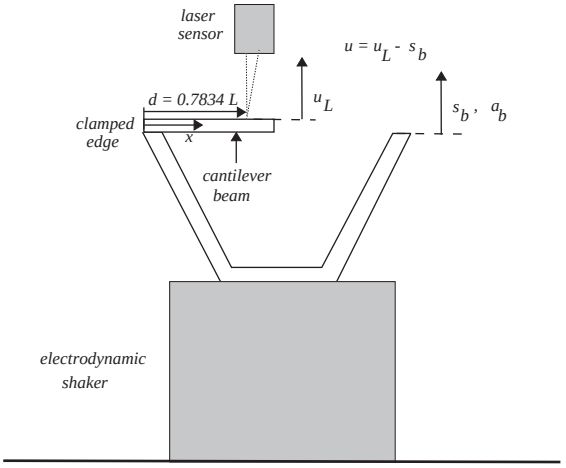

Fig. 7. Set-up of the cantilever beam, the support and the shaker for measurement of Young's modulus.

be able to carry out several tests at different temperatures. Fig. 2 (B) shows a diagram of the whole measurement system, which contains the same temperature controlled chamber used for the tests on the Poisson ratio.

A specifically designed aluminium cup supports the specimen, which is glued to the cup at one extremity, so as to implement a cantilever beam. The choice of a cantilever beam, i.e., a beam with clamped–free boundary conditions, turned out to be the optimal one for this kind of tests after many years of tests where different boundary conditions were tried.

The specimen is excited by the shaker, and it is subject to a seismic bending force. According to Eq. (14), in order to determine an expression for Young's modulus of the specimen, the absolute displacement of the specimen itself, as well as the acceleration of the support are required. The latter is measured by an accelerometer set on the edge of the support; the former is provided by a laser sensor, which measures the absolute displacement of the specimen at the point where the amplitude of the second eigenmode is null (for a cantilever beam, at a distance from the fastened

Fig. 8. Photograph of the experimental set-up for measurement of Young's modulus.

extremity equal to 0.7834 times the free length of the beam). In this way the error made by approximating the whole eigenfunction expansion with the first eigenmode only is reduced (less than 0.4% in the frequency range used in the experiment).

The laser sensor is employed in the experimental apparatus is an OptoNCDT series 1605-2 by MicroEpsilon, that has a resolution of 0.5 μm on a measurement range of ± 1 mm. The main advantage of using a contactless sensor to measure the small displacements of the beam lies in the fact that no perturbation of the measurement is introduced (conversely, using a strain gauge glued to the specimen did locally change the stiffness of the material, as proved by some experimental tests made in the earlier stages of the work).

A second cantilever beam of the same material, identical to the one tested, but instrumented with a strain gauge, was mounted onto the support, in order to provide a feedback signal to the sweep controller that drives the shaker. The control value of the longitudinal strain was set at 20 μm/m.

Finally, the dynamic analyzer is a dedicated software, made by the authors, running on a PC in a Labview environment. The experimental signals are input to the PC through a National

Instrument AT-A2150 I/O board, and then they are analyzed and elaborated by the software, so as to get curves for both absolute values and phase angles of Young's modulus at different temperatures.

7. Application of the reduced variables method to determine the master curve for Young's modulus

Figs. 9 and 10 show the experimental results of the measurement of Young's modulus for the viscoelastic material tested (absolute values and phase angles, respectively). In Fig. 10 some curves have been deleted for sake of clarity.

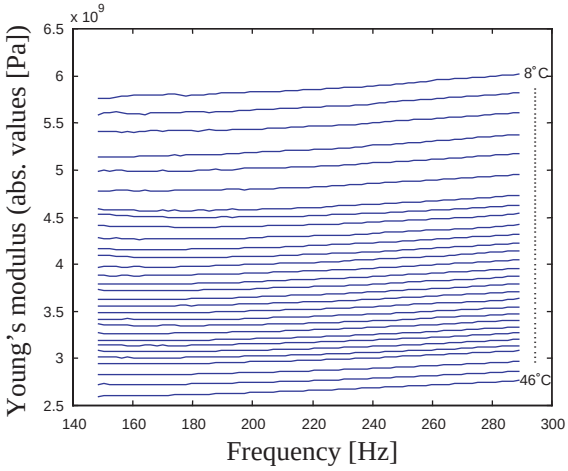

Fig. 9. Absolute values of Young's modulus at different temperatures.

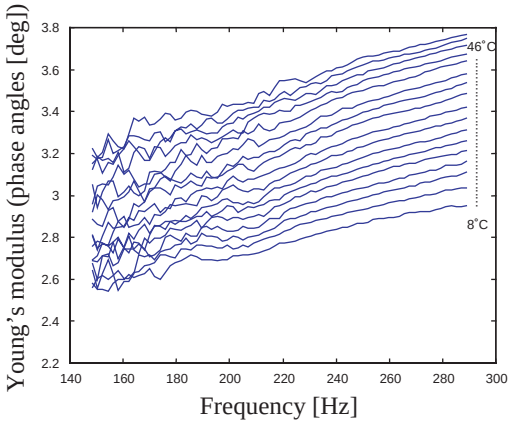

Fig. 10. Phase angles of Young's modulus at different temperatures.

The procedure to build the master curve for Young's modulus is the same used for the Poisson ratio. It is based on the approximate causality condition and on its derivative, which for Young's modulus are, respectively,

$$\varphi(E(\mathrm{i}\omega)) \cong \frac{\pi}{2}\frac{\mathrm{d}\,\log|E(\mathrm{i}\omega)|}{\mathrm{d}\,\log\,\omega}, \tag{19}$$

$$\frac{\mathrm{d}\varphi(E(\mathrm{i}\omega))}{\mathrm{d}\,\log\,\omega} \cong \frac{\pi}{2}\frac{\mathrm{d}^2\,\log|E(\mathrm{i}\omega)|}{\mathrm{d}(\log\,\omega)^2}, \tag{20}$$

where $\varphi(E(\mathrm{i}\omega))$ is the phase angle of the complex Young's modulus $E(\mathrm{i}\omega)$. Then, the reduced variables method produces a master curve for Young's modulus of the considered material.

The steps of the iterative procedure used to get the master curve for Young's modulus are the same as those listed in Section 5 for the Poisson ratio, with the substitution of ν with E. In this way, the initial versions of the master curves for the absolute values and for the phase angles could be obtained. Then, on applying the procedure to the experimental data recorded, only three iterations were needed to obtain stable values for the coefficients of the parabolas and for the shifts. At this point, reliable shifts are available to build the master curve. Fig. 11 represents the shifts obtained at the end of the iteration as a continuous function of the temperature, being $T_0 = 319\,\mathrm{K}$ the reference temperature.

The values obtained for the coefficients of the WLF equation are: $c_1^0 = 19.73$ and $c_2^0 = 119.40$, which are in reasonable agreement with the values reported in the literature for Young's modulus or for the shear modulus of materials similar to that of the tested specimen, as well as with the values of c_1^0 and c_2^0 obtained from the calculation of the Poisson ratio. The coefficient c_1^0 and c_2^0 could then be used to get the master curves for the absolute value (Fig. 12) and for the phase angle (Fig. 13) of the complex Young's modulus in a very broad frequency range (from 10^2 to 10^8 Hz). It can be seen from Fig. 12 that the behaviour of the absolute value of Young's modulus is in good agreement with the theory, namely it increases with frequency. As for the Poisson ratio, the result

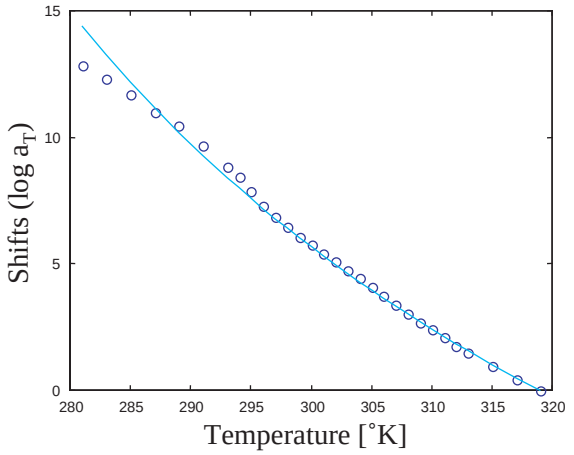

Fig. 11. Plot of the shifts of the curves of Young's modulus as a continuous function of the temperature (according to the WLF equation for a reference temperature $T_0 = 319\,\mathrm{K}$) and experimental values of $\log a_T$ at each temperature.

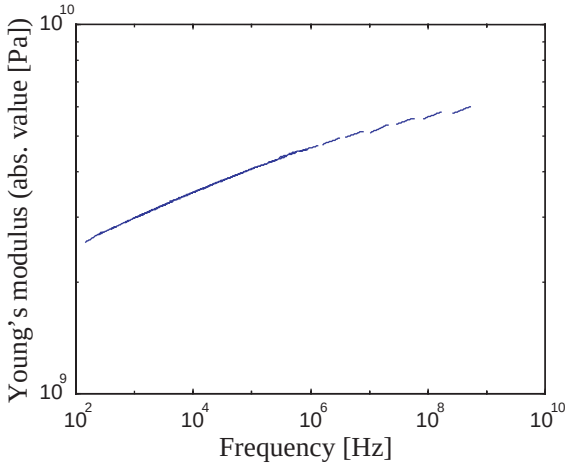

Fig. 12. Master curve for the absolute value of Young's modulus.

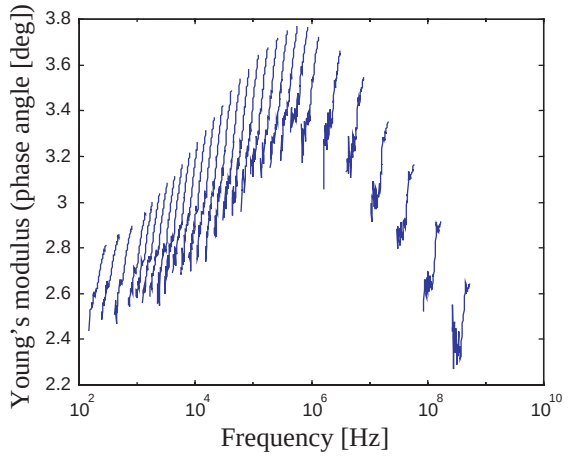

Fig. 13. Master curve for the phase angle of Young's modulus.

for the phase angle is less clear, because the value of the phase angle of the tested material is very small (a few degrees), hence the measurement noise could definitely affect the result. However, it can be noted that the maximum of the master curve of the phase angle corresponds to the change of curvature of the master curve of the absolute values, thus being in agreement with the causality relation and the theory of viscoelasticity.

8. Conclusions

An experimental method for determining the Poisson ratio and the complex dynamic Young's modulus in a small beam subject to seismic excitation was presented in this paper, together with the theoretical background of such a technique.

The same experimental device has basically been used for both tests: a beam-like specimen was instrumented and collocated into a temperature-controlled chamber. The specimen was excited by means of an electrodynamic shaker. To get the Poisson ratio the longitudinal and the transversal deformations have been measured by strain gauges, whereas the vertical displacement of the specimen and the acceleration of the support have been measured to get Young's modulus.

The experimental set-up has been described in detail, and the experimental curves of the Poisson ratio and of Young's modulus at different temperatures have been reported. Each set of curves at different temperatures was then gathered into a unique master curve by using the reduced variables method. The two master curves, respectively, represent the Poisson ratio and Young's modulus for the tested material in a very broad frequency range. It is worth noting that the improved reduced variables method presented in the paper could also be applied to results obtained using other experimental methods.

References

[1] R.M. Christensen, *Theory of Viscoelasticity*, Academic Press, London, 1982.
[2] J.D. Ferry, *Viscoelastic Property of Polymers*, Wiley, Chichester, 1970.
[3] A.D. Nashif, D.I.G. Jones, J.P. Henderson, *Vibration Damping*, Wiley, Chichester, 1985.
[4] W.G. Gottenberg, R.M. Christensen, An experiment for determination of the mechanical property in shear for a linear, isotropic viscoelastic solid, *International Journal of Engineering Science* 2 (1964) 45–57.
[5] T. Pritz, Transfer function method for investigating the complex modulus of acoustic materials: spring-like specimen, *Journal of Sound and Vibration* 72 (3) (1980) 317–341.
[6] T. Pritz, Transfer function method for investigating the complex modulus of acoustic materials: rod-like specimen, *Journal of Sound and Vibration* 81 (3) (1982) 359–376.
[7] T. Pritz, Dynamic strain of a longitudinally vibrating viscoelastic rod with an end mass, *Journal of Sound and Vibration* 85 (2) (1982) 151–167.
[8] T. Pritz, Dynamic Young's modulus and loss factor of plastic foams for impact sound isolation, *Journal of Sound and Vibration* 178 (3) (1994) 315–322.
[9] B.P. Holownia, Experimental measurement of dynamic bulk modulus using holography, *Rubber Chemistry and Technology* 58 (1985) 258–268.
[10] B.P. Holownia, A.C. Rowland, Measurement of dynamic bulk modulus and phase angle using ESPI, *Rubber Chemistry and Technology* 59 (1986) 223–232.
[11] S. Sim, K.J. Kim, A method to determine the complex modulus and Poisson's ratio of viscoelastic materials for FEM applications, *Journal of Sound and Vibration* 141 (1) (1990) 71–82.
[12] S. Ödeen, B. Lundberg, Determination of complex modulus from measured end-point accelerations of an impacted rod specimen, *Journal of Sound and Vibration* 165 (1) (1993) 1–8.
[13] I.N. Trendafilova, S. Ödeen, B. Lundberg, Identification of viscoelastic materials from electro-optical displacement measurements at two sections of an impacted rod specimen, *European Journal of Mechanics A: Solids* 13 (6) (1994) 793–802.
[14] C. Hakan Gür, B. Aydinmakina, Non-destructive characterisation of nodular cast irons by ultrasonic method, *Proceedings of the 15th World Conference on Non-Destructive Testing*, Rome, 2000, pp. 269–275.
[15] D.E. Bray, Current directions of the ultrasonic stress measurement techniques, *Proceedings of the 15th World Conference on Non-Destructive Testing*, Rome, 2000, pp. 1209–1215.
[16] M. Giovagnoni, On the direct measurement of the dynamic Poisson's ratio, *Mechanics of Materials* 17 (1994) 33–46.
[17] R. Caracciolo, M. Giovagnoni, Frequency dependence of Poisson's ratio using the method of reduced variables, *Mechanics of Materials* 24 (1996) 75–85.

[18] R. Caracciolo, A. Gasparetto, M. Giovagnoni, An experimental method to determine Poisson's ratio in a small beam subject to seismic excitation, *Proceedings of the 16th ASME Biennial Conference on Mechanical Vibration and Noise*, Sacramento, CA, 1997.

[19] R. Caracciolo, A. Gasparetto, M. Giovagnoni, Measurement of the isotropic dynamic Young's modulus in a seismically excited cantilever beam using a laser sensor, *Journal of Sound and Vibration* 231 (5) (2000) 1339–1353.

[20] R. Caracciolo, A. Gasparetto, M. Giovagnoni, Application of causality check and of the reduced variables method for experimental determination of Young's modulus of a viscoelastic material, *Mechanics of Materials* 33 (2001) 693–703.

[21] T. Pritz, Verification of local Kramers–Krönig relations for complex modulus by means of fractional derivative model, *Journal of Sound and Vibration* 228 (5) (1999) 1145–1165.